Supplementary Materials: Quantitative Systems Pharmacology Modeling Framework of Autophagy in Tuberculosis: Application to Adjunctive Metformin Host-Directed Therapy

Contents

1 Model Development Methods and the Final Model Code

1.1 Pharmacokinetic Models

PK models for HRZE were reproduced from literature-based population pharmacokinetic (PopPK) models [1, 2]. HRZE intra- and extra-cellular lung concentrations were predicted by applying plasma to lung alveolar cells (AC) and plasma to lung epithelial lining fluid (ELF) ratios obtained from literature [3].

To predict lung concentrations of metformin, we developed a minimal physiologically based pharmacokinetic (mPBPK) model including a lung compartment (Figure1). The model equations were kept similar to previous mPBPK model with lung compartment [4] for Ivermectin, and parameter relevant to blood plasma to lung partition was obtained from a published metformin PBPK model [5].

Figure 1: Observed vs. Predicted: Metformin Pharmacokinetics

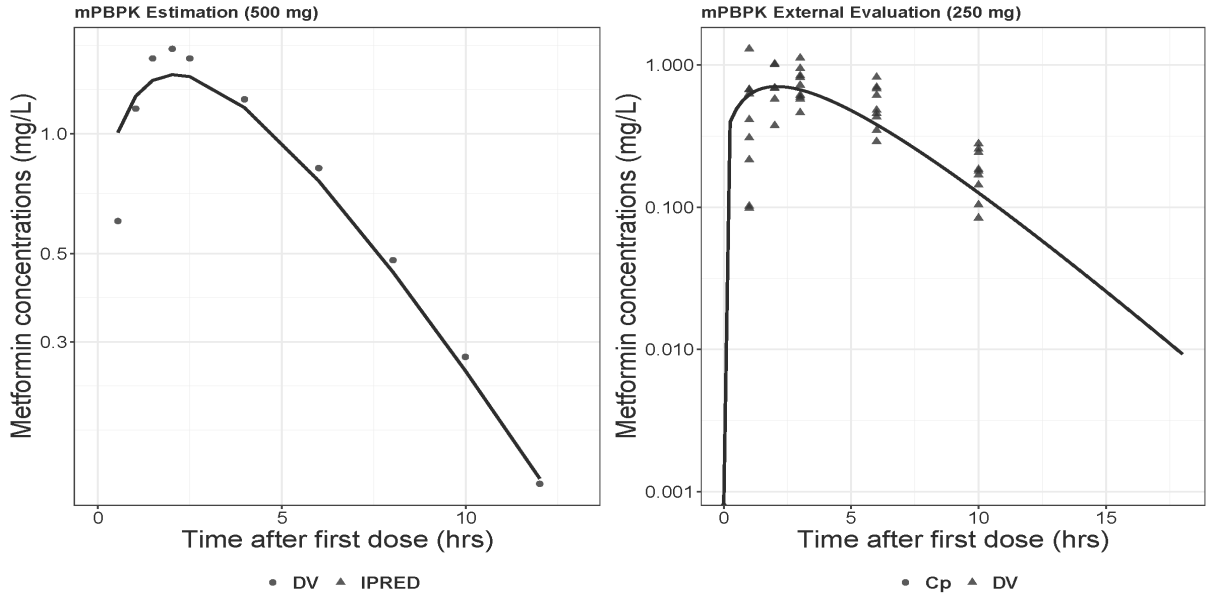

1.2 TB Host-Immune Response Model and Pharmacodynamics of Standard Antibiotics

A published model that captured dynamics of the host immune response following Mtb infection was reproduced using RxODE [6]. An update was made to the model for addition of the turn-over of IL-1b and IL-1b-mediated bacterial killing. The parameters of IL-1b turn-over were obtained the literature [7, 8], and the IL-1b-mediated bacterial killing rate was optimized by fitting a simplified model to in vitro digitized data from literature [9]. Model fitting output is shown in Figure1.2.

Figure 2: Observed vs. Predicted: Percent Growth Inhibition of Mtb in Macrophage Cell Cultures at Various IL-1b Concentrations

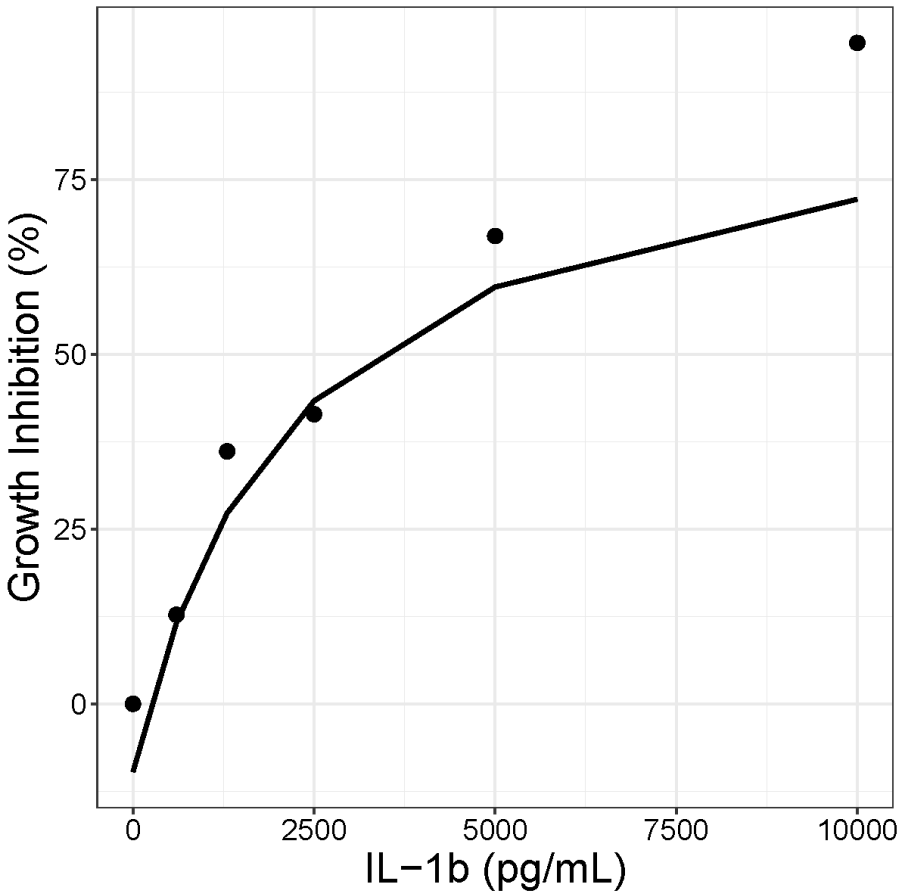

1.2.1 Fast- and Slow- Growth Phases of Mtb

In our model, we included two Mtb growth phase, fast and slow. We used the slow or persistent state bacterial growth rate estimates same as the growth rate values from the reproduced TB host immune response model [6]. The growth rate estimates for the initial fast or log-growth phase were optimized using data from mice infection experiment [10]. Prior to parameter optimization using mice infection data, the TB host-immune response model needed to be scaled from humans to mice. Lung volume difference between the species was incorporated. Output from the parameter optimization is shown in Figure3. The switch from fast to slow growth rates was empirically set to 21 days post-infection based on mice infection experimental results [11, 10].

Figure 3: Observed vs. Predicted: Bacterial Load in Mice Infected with Mtb

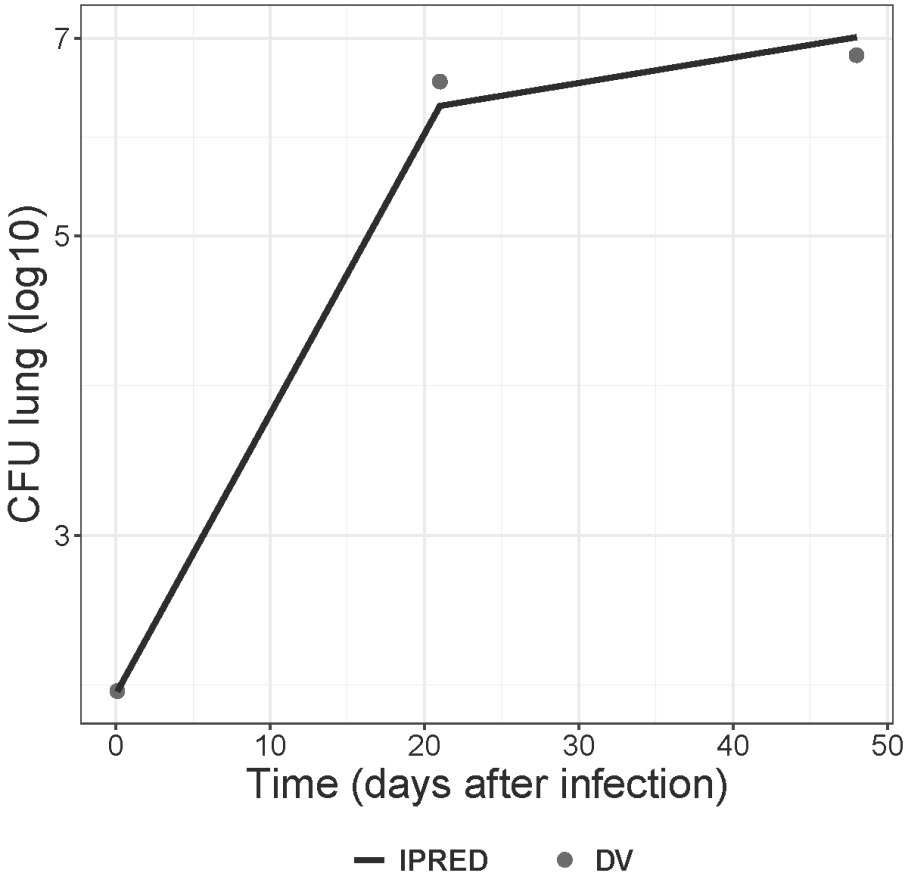

PD models for bactericidal and bacteriostatic effects of HRZE were reproduced from the literature [12].

1.3 Autophagy Model and Pharmacodynamics of Metformin

Next, an AMPK-mTOR cell signalling network model from literature was reproduced in RxODE [13]. The model then was updated to include various Mtb- and autophagy-related components.

1.3.1 Effect of Mtb on Autophagy Inhibition

To simulate the effects of Mtb infection on AMPK-mTOR signalling, a dataset containing ratios of differentially expressed genes in lungs of Mtb infected vs. uninfected mice [14] was examined for proteins of interest, i.e., the ones included in AMPK-mTOR signaling model. Gene AKT3 was found to be induced 1.38-fold in Mtb-infected vs. uninfected mice. This was added as a proportional scaling factor on AKT production rate in the model to represent Mtb presence. Thus, the effect of Mtb-mediated AKT induction on rest of the markers, including AMPK and mTORC1 can be simulated. It was assumed that Mtb does not act directly on AMPK or mTORC1, as their relevant genes were not found in the evaluated dataset. Mtb effect on these downstream proteins can assumed to be an indirect effect of AKT activation. Comparison of model-predicted fold change in Mtb infected vs. uninfected state is shown in table below. Time course impact of Mtb load on AMPK-mTOR signalling was not evaluated in this work due to limitations of the available data.

	Protein	Fold change (Infected vs. Uninfected)
1	Akt_pS473	0.28
2	Akt_pT308	0.32
3	AMPK_pT172	-0.04
4	IR_beta_pY1146	-0.00
5	IR_beta_refractory	-0.00
6	IRS1_p	-0.04
7	IRS1_pS636	0.00
8	mTORC1_pS2448	0.12
9	mTORC2_pS2481	-0.00
10	p70S6K_pT389	0.04
11	PI3K_variant_p	-0.00
12	PRAS40_pS183	0.06
13	PRAS40_pT246	0.30
14	TSC1_TSC2_pS1387	-0.17
15	TSC1_TSC2_pT1462	0.15

The autophagy at baseline (at time of Mtb infection) was set to 100% to represent healthy state prior to infection. The change in autophagy due to mTORC1 activation was described by a direct effect saturable Emax model. Maximum effect of mTORC1 on autophagy was optimized by fitting the model to in vitro infection experiments in absence and presence of metformin (Figure4) [14]. mTORC1 levels at which 50% of maximum autophagy inhibition occurs was set arbitrarily to median value from the simulated range for mTORC1.

1.3.2 Effect of Autophagy on Bacterial Clearance

Autophagy-mediated intracellular bacterial killing was incorporated within the differential equations for intracellular bacteria and the rate was optimized by fitting the model to in vitro infection experiments in absence and presence of metformin [14]. Impact of autophagy on phagocytosis was incorporated by adding a linear coefficient on extracellular to intracellular bacterial uptake parameter, and the coefficient slope was assumed 1. The inhibitory effect of metformin on mTORC1 phosphorylation was incorporated using an indirect effect saturable Emax model, and the parameters were obtained from the literature [15, 16]. Some underpredictions of metformin effects at higher concentrations were noted in the model fit (Figure4). It can be hypothesized that metformin may act on multiple proteins within the AMPK-mTOR pathway. The current model only included inhibitory effect of metformin on mTORC1.

Figure 4: Observed vs. Predicted: Mtb Surival in Macrophage Cell Cultures Treated with Metformin

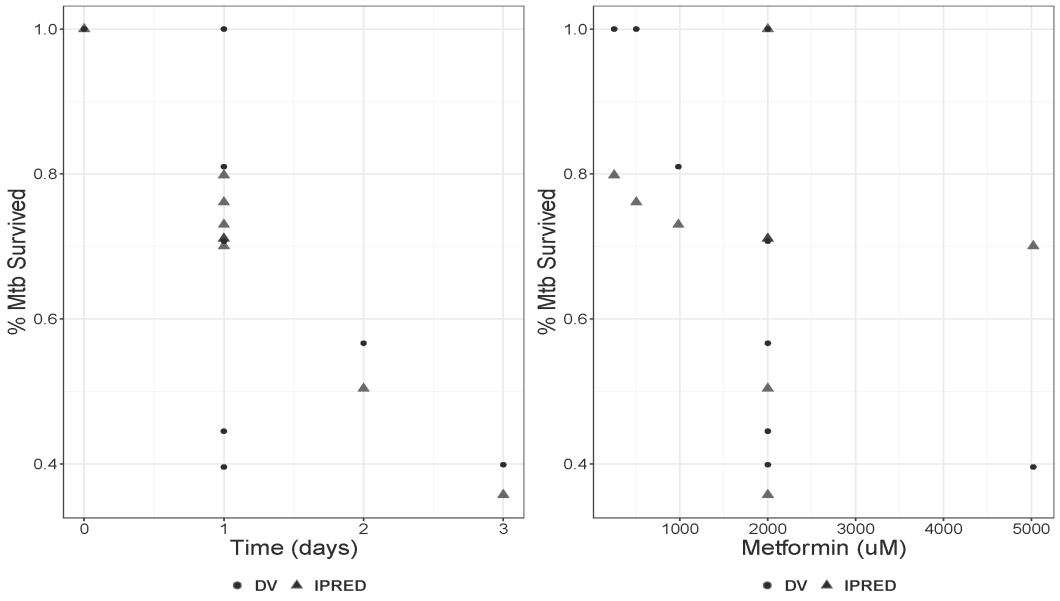

The updated TB host immune response model and autophagy models were then combined to simulate the effects of adjunctive treatment with metformin in a typical TB patient. Few updates were made to the combined model to capture additional mechanistic details.

1.3.3 Effect of AMPK-mTORC1 Signalling on IFN-y

To capture the effects of AMPK-mTORC1 signaling on production of IFN-y, AMPK-mediated inhibition of IFN-y production by infected macrophage was added [17]. The maximum inhibition of IFN-y on production by infected macrophage was set to 50%, the phosphorylated AMPK concentrations at which the inhibition is 50% was set arbitrarily to median AMPK value from the simulated range. It should be noted that additional IFN-y production terms, i.e., T-cell mediated production, remain unchanged from the original equations.

1.4 Final TB-Autophagy QSP Model RxODE Code

```
##Time in hours
mod1 <- RxODE({

  #Rifampin PK (Svensson 2018, PMID:28653479)
  enzRIF(0) = 1 ;
  VmaxRIF = VmaxRIF*(WT/70)^0.75 ;
  VRIF = VRIF*(WT/70) ;
  BIO = 1*(1 + (FMAXRIF*(DOSERIF-450))/(ED50RIF+(DOSERIF-450))) ;
  d/dt(depotRIF) = transit(NNRIF,MTTRIF,BIO) - kaRIF*depotRIF  ;
  d/dt(centRIF) = kaRIF*depotRIF -
  ((VmaxRIF/(KmRIF+(centRIF/VRIF)))/VRIF)*centRIF*enzRIF  ;
  d/dt(enzRIF) = KENZRIF*(1+(EmIRIF*(centRIF/VRIF))/(EC50IRIF+(centRIF/VRIF))) -
  KENZRIF*enzRIF  ;
  CpRIF = centRIF/VRIF ;
  CinRIF = CpRIF*ACRIF ;
  CexRIF = CpRIF*ELFRIF ;
  CnliR =  CinRIF ;
  CnlR = CexRIF ;

  #Isoniazid PK (Denti 2015, PMID:26501782)
```

```
 if(ACEStatus==0) {CLINH=CLRINH ;} else {CLINH=CLSINH ;}
 CLINH = CLINH*(WT/51.9)^0.75 ;
 QINH = QINH*(WT/51.9)^0.75 ;
 VINH = VINH*(WT/51.9)   ;
 V2INH = V2INH*(WT/51.9) ;
 d/dt(depotINH) = -transit(NNINH,MTTINH,1) ;
 d/dt(centINH) = transit(NNINH,MTTINH,1) - (CLINH/VINH)*centINH -
 (QINH/VINH)*centINH + (QINH/V2INH)*periINH ;
 d/dt(periINH) = (QINH/VINH)*centINH - (QINH/V2INH)*periINH ;
 CpINH = centINH/VINH ;
 CinINH = CpINH*ACINH ;
 CexINH = CpINH*ELFINH ;
 CnliI =  CinINH  ;
 CnlI = CexINH    ;

 #Pyrazinamide PK (Denti 2015, PMID:26501782)
 CLPYZ = CLPYZ*(WT/51.9)^0.75 ;
 VPYZ = VPYZ*(WT/51.9)   ;
 d/dt(depotPYZ) = -transit(NNPYZ,MTTPYZ,1) ;
 d/dt(centPYZ) = transit(NNPYZ,MTTPYZ,1) - (CLPYZ/VPYZ)*centPYZ ;
 CpPYZ = centPYZ/VPYZ ;
 CinPYZ = CpPYZ*ACPYZ ;
 CexPYZ = CpPYZ*ELFPYZ ;
 CnliP = CinPYZ ;
 CnlP = CexPYZ  ;

 #Ethambutol PK (Denti 2015, PMID:26501782)
 CLETH = CLETH*(WT/51.9)^0.75 ;
 QETH = QETH*(WT/51.9)^0.75 ;
 VETH = VETH*(WT/51.9)   ;
 V2ETH = V2ETH*(WT/51.9) ;
 d/dt(depotETH) = -transit(NNETH,MTTETH,1) ;
 d/dt(centETH) = transit(NNETH,MTTETH,1) - (CLETH/VETH)*centETH -
 (QETH/VETH)*centETH + (QETH/V2ETH)*periETH ;
 d/dt(periETH) = (QETH/VETH)*centETH - (QETH/V2ETH)*periETH ;
 CpETH = centETH/VETH ;
 CinETH = CpETH*ACETH ;
 CexETH = CpETH*ELFETH ;
 CnliE = CinETH ;
 CnlE = CexETH  ;

if(t<2*24){
   kmaxeR = kmaxeR1 ;
   kmaxeI = kmaxeI1 ;
   kmaxeP = kmaxeP1 ;
   kmaxeE = kmaxeE1 ;
   kmaxiR = kmaxiR1 ;
   kmaxiI = kmaxiI1 ;
   kmaxiP = kmaxiP1 ;
  kmaxiE = kmaxiE1 ;
 } else {
   if(t>15*24){
     kmaxeR = kmaxeR15 ;
     kmaxeI = kmaxeI15 ;
   kmaxeP = kmaxeP15 ;
 kmaxeE = kmaxeE15 ;
 kmaxiR = kmaxiR15 ;
 kmaxiI = kmaxiI15 ;
  kmaxiP = kmaxiP15 ;
```

```
    kmaxiE = kmaxiE15 ;
   } else
   {
      kmaxeR = kmaxeR2 ;
      kmaxeI = kmaxeI2 ;
      kmaxeP = kmaxeP2 ;
      kmaxeE = kmaxeE2 ;
      kmaxiR = kmaxiR2 ;
      kmaxiI = kmaxiI2 ;
      kmaxiP = kmaxiP2 ;
      kmaxiE = kmaxiE2 ;
     }
   }


  #Extracellular Mtb bacteria
  if(CnlR > EC50R1){
    statR = 1
  } else {statR = (1- (1/(1 + (EC50R1/CnlR)^GR1)))}

  if(CnlI > EC50I1){
    statI = 1
  } else {statI = (1- (1/(1 + (EC50I1/CnlI)^GI1)))}

  if(CnlP > EC50P1){
    statP = 1
  } else {statP = (1- (1/(1 + (EC50P1/CnlP)^GP1)))}

  if(CnlE > EC50E1){
    statE = 1
  } else {statE = (1- (1/(1 + (EC50E1/CnlE)^GE1)))}

  killR = kmaxeR*(1/(1+(EC50R/CnlR)^GR)) ;
  killI = kmaxeI*(1/(1+(EC50I/CnlI)^GI)) ;
  killP = kmaxeP*(1/(1+(EC50P/CnlP)^GP)) ;
  killE = kmaxeE*(1/(1+(EC50E/CnlE)^GE)) ;

  if(CnliR > EC50R1){
    statiR = 1
} else {statiR = (1- (1/(1 + (EC50R1/CnliR)^GR1)))}

  if(CnliI > EC50I1){
    statiI = 1
  } else {statiI = (1- (1/(1 + (EC50I1/CnliI)^GI1)))}

  if(CnliP > EC50P1){
    statiP = 1
  } else {statiP = (1- (1/(1 + (EC50P1/CnliP)^GP1)))}

  if(CnliE > EC50E1){
    statiE = 1
  } else {statiE = (1- (1/(1 + (EC50E1/CnliE)^GE1)))}

  killiR = kmaxiR*(1/(1+(EC50R/CnliR)^GR)) ;
  killiI = kmaxiI*(1/(1+(EC50I/CnliI)^GI)) ;
  killiP = kmaxiP*(1/(1+(EC50P/CnliP)^GP)) ;
  killiE = kmaxiE*(1/(1+(EC50E/CnliE)^GE)) ;
})
```

```
##Time in days
##Input should include daily median of killxx and statxx

mod2 <- RxODE({

#Metformin mPBPK
#Optimized some parameters (see S1)
#Codes adapted from Jermain 2020
 ka = ka*24 ;
 CL = CL*24 ;
 Qco = Qco*24 ;
  d/dt(metdepot) = -ka*metdepot ;
  d/dt(metcent) = ka*metdepot -(CL/VpMET)*metcent + metlung*Qco/(Vl*Kplung) - metcent*Qco/VpMET +
    metoth*Qco*FRC/(Voth*Kpoth) - metcent*Qco*FRC/VpMET ;
  d/dt(metlung) = metcent*Qco/VpMET - metlung*Qco/(Vl*Kplung) ;
  d/dt(metoth) = metcent*Qco*FRC/VpMET - metoth*Qco*FRC/(Voth*Kpoth)  ;
  CpMET = metcent/VpMET       ;
  ClMET = metlung/Vl       ;
  MET = ClMET*1000/129 ; # mg/L to umol/L

#Bacterial growth rates
  if(t<=21) {
  A19 = A191;
  A20 = A201 ;} else {
  A19 = A192;
  A20 = A202 ;
  }

#AKT3 gene fold change (infected/uninfected) = 1.38 #Singhal 2014
  if(Bi>=1) {MTBY=1 ;} else {MTBY = 0 ;}
  if(MTBY==1) {AKT3FC = 1.38 ;} else {AKT3FC = 1;}

  mtor = mTORC1_pS2448 ;

#Autophagy assumed 100% for healthy state (at time of infection)
#Effect of mtor on autophagy
  autop = 100 - (mtor*Smtorauto/(mtor+S50torauto))   ;

#Assumed Emax=1, i.e., full inhibition can happen depending on concentrations
  METeff = (1 - (MET/(E50MET+MET)))  ;

#minimum autophagy 30%, slope assumed 1 and centered at 30
#Effect of autophagy on phagocytosis (extra- to intra- engulfment)
 k2stim = SLPk2autop*autop/30 ;

######## Sonntag 2012 Model (PMID: 22452783) ##########
# SBML file was obtained from supplementary materials of the paper.
# Converted to ODE format using IQsbml package from Intiquan.
# Convered ODE to RxODE format manually
# Rates converted to 1/days

  #IR_beta_phosphorylation_by_Insulin
  reaction_1 = P1*IR_beta*Insulin      ;

  #IR_beta_pY1146_dephosphorylation
  reaction_2 = P2 * IR_beta_pY1146     ;

  #IR_beta_ready
  reaction_3 = P3 * IR_beta_refractory ;
```

```
#IRS1_phosphorylation_by_IR_beta_pY1146
reaction_4 = P4*IRS1*IR_beta_pY1146  ;

# IRS1_p_phosphorylation_by_p70S6K_pT389
reaction_5 = P5*IRS1_p*p70S6K_pT389   ;

# IRS1_pS636_dephosphorylation
reaction_6 = P6 * IRS1_pS636          ;

# AMPK_T172_phosphorylation
reaction_7 = P7*AMPK*IRS1_p         ;

# AMPK_pT172_dephosphorylation
reaction_8 = P8 * AMPK_pT172          ;

# Akt_pT308_dephosphorylation
reaction_9 = P9 * Akt_pT308            ;

# Akt_pS473_dephosphorylation
reaction_10 = P10 * Akt_pS473          ;

# Akt_S473_phosphorylation_by_mTORC2_pS2481_n_IRS1_p
# Added AKT3FC here
reaction_11 = P11*Akt_S473*mTORC2_pS2481*IRS1_p*AKT3FC   ;

# Akt_T308_phosphorylation_by_IRS1_p
reaction_12 = P12*Akt_T308*IRS1_p*AKT3FC                 ;

# mTORC1_pS2448_dephosphorylation_by_TSC1_TSC2_pS1387
reaction_13 = P13*mTORC1_pS2448*TSC1_TSC2_pS1387   ;

# mTORC1_S2448_activation_by_Amino_Acids
# Added METeff here
reaction_14 = P14*mTORC1*Amino_Acids*METeff        ;

# mTORC2_pS2481_dephosphorylation
reaction_15 = P15 * mTORC2_pS2481                  ;

# mTORC2_S2481_phosphorylation_by_PI3K_variant_p
reaction_16 = P16*mTORC2*PI3K_variant_p             ;

# p70S6K_pT389_dephosphorylation
reaction_17 = P17 * p70S6K_pT389                ;

# p70S6K_T389_phosphorylation_by_mTORC1_pS2448
reaction_18 = P18*p70S6K*mTORC1_pS2448          ;

# PRAS40_pS183_dephosphorylation
reaction_19 = P19 * PRAS40_pS183                 ;

# PRAS40_pT246_dephosphorylation
reaction_20 = P20 * PRAS40_pT246                 ;

# PRAS40_S183_phosphorylation_by_mTORC1_pS2448
reaction_21 = P21*PRAS40_S183*mTORC1_pS2448        ;

# PRAS40_T246_phosphorylation_by_Akt_pT308
reaction_22 = P22*PRAS40_T246*Akt_pT308            ;
```

```
# TSC1_TSC2_S1387_phosphorylation_by_AMPK_pT172
reaction_23 = P23*TSC1_TSC2_pT1462*AMPK_pT172       ;

# TSC1_TSC2_T1462_phosphorylation_by_Akt_pT308
reaction_24 = P24*TSC1_TSC2_pS1387*Akt_pT308       ;

# PI3K_variant_p_dephosphorylation
reaction_25 = P25 * PI3K_variant_p                 ;

# PI3K_variant_phosphorylation_by_IR_beta_pY1146
reaction_26 = P26*PI3K_variant*IR_beta_pY1146       ;

d/dt(Amino_Acids) = 0 ; #Steady input
d/dt(Insulin) = 0 ;     #Steady input
d/dt(IR_beta) = (-reaction_1+reaction_3)      ;
d/dt(IR_beta_pY1146) = (+reaction_1-reaction_2)      ;
d/dt(IR_beta_refractory) = (+reaction_2-reaction_3)      ;
d/dt(IRS1) = (-reaction_4+reaction_6)      ;
d/dt(IRS1_p) = (+reaction_4-reaction_5)      ;
d/dt(IRS1_pS636) = (+reaction_5-reaction_6)      ;
d/dt(AMPK) = (-reaction_7+reaction_8)      ;
d/dt(AMPK_pT172) = (+reaction_7-reaction_8)      ;
d/dt(Akt_T308) = (+reaction_9-reaction_12)      ;
d/dt(Akt_pT308) = (-reaction_9+reaction_12)      ;
d/dt(Akt_S473) = (+reaction_10-reaction_11)      ;
d/dt(Akt_pS473) = (-reaction_10+reaction_11)      ;
d/dt(mTORC1) = (+reaction_13-reaction_14)      ;
d/dt(mTORC1_pS2448) = (-reaction_13+reaction_14)      ;
d/dt(mTORC2) = (+reaction_15-reaction_16)      ;
d/dt(mTORC2_pS2481) = (-reaction_15+reaction_16)      ;
d/dt(p70S6K) = (+reaction_17-reaction_18)      ;
d/dt(p70S6K_pT389) = (-reaction_17+reaction_18)      ;
d/dt(PRAS40_T246) = (+reaction_20-reaction_22)      ;
d/dt(PRAS40_pT246) = (-reaction_20+reaction_22)      ;
d/dt(PRAS40_S183) = (+reaction_19-reaction_21)      ;
d/dt(PRAS40_pS183) = (-reaction_19+reaction_21)      ;
d/dt(TSC1_TSC2_pT1462) = (-reaction_23+reaction_24)      ;
d/dt(TSC1_TSC2_pS1387) = (+reaction_23-reaction_24)      ;
d/dt(PI3K_variant) = (+reaction_25-reaction_26)      ;
d/dt(PI3K_variant_p) = (-reaction_25+reaction_26)      ;

#Please see Sud 2006 (PMID: 16547267) for description of the base TB model
# + additions (IL-1b, kautop)

par1 = ((Tc*(T1/(T1+cT1)))+(w1*T1))/Mi ;

#Intracellular bacteria (Bi)
d/dt(Bi) = Bi*((A19*(1-(Bi^2/((Bi^2)+(N*Mi)^2)))*statiR*statiI*statiP*statiE) -
                (killiR + killiI + killiP + killiE)) +
  k2*(N/2)*Mr*(Be/(Be+c9))*k2stim -
  k17*N*Mi*(Bi^2/((Bi^2)+(N*Mi)^2)) -
  k14a*N*Mi*(((Tc+(w3*T1))/Mi)/(((Tc+(w3*T1))/Mi)+c4)) -
  k14b*N*Mi*(Fa/(Fa + f9*I10 + s4b)) -
  k14x*N*Mi*(IL1b/(IL1b + f9*I10 + s4x)) -  # IL-1b added (see S1, structure same as TNF-a)
  k52*N*Mi*(par1/(par1 + c52)) - Mui*Bi - kautop*Bi*autop; #autophagy effect added

#Extracellular bacteria (Be)
d/dt(Be) =  Be*((A20*(1-(Be/5e+8))*statR*statI*statP*statE) - (killR + killI + killP + killE)) +
```

```
  k17*N*Mi*(Bi^2/((Bi^2)+(N*Mi)^2)) - k2*(N/2)*Mr*(Be/(Be+c9))*k2stim + #k2stim applied here
  k14a*N*Nfracc*Mi*(((Tc+(w3*T1))/Mi)/(((Tc+(w3*T1))/Mi)+c4)) +
  k14b*N*Nfraca*Mi*(Fa/(Fa + f9*I10 + s4b)) +
  k14x*N*Nfraca*Mi*(IL1b/(IL1b + f9*I10 + s4x)) - # IL-1b added (see S1, structure same as TNF-a)
  k15*Ma*Be - k18*Mr*Be +  Mui*Bi ;

Bt = Bi + Be          ;

#Resident macrophage
d/dt(Mr) = srm + A4a*(Ma+w2*Mi) + sr4b*(Fa/(Fa+(f8*I10)+s4b)) - k2*Mr*(Be/(Be+c9))*k2stim -
  k3*Mr*(Iy/(Iy+(f1*I4)+s1))*((Bt + B*(Fa+IL1b))/(Bt + B*(Fa+IL1b) + c8)) -
  MuMr*Mr   ;

#Infected macrophage
d/dt(Mi) = k2*Mr*(Be/(Be+c9))*k2stim - k17*Mi*(Bi^2/((Bi^2)+(N*Mi)^2)) -
  k14a*Mi*(((Tc+(w3*T1))/Mi)/(((Tc+(w3*T1))/Mi) +c4)) -
  k14b*Mi*(Fa/(Fa+(f9*I10)+s4b)) -
  k14x*Mi*(IL1b/(IL1b+(f9*I10)+s4x)) -
  k52*N*Mi*(par1/(par1 + c52)) -
  MuMi*Mi             ;

#Activated macrophage
d/dt(Ma) = k3*Mr*(Iy/(Iy+(f1*I4)+s1))*((Bt + B*(Fa+IL1b))/(Bt + B*(Fa+IL1b) + c8)) -
  k4*Ma*(I10/(I10+s8)) - MuMa*Ma             ;

#Naive T cells
d/dt(T0) = A1a*(Ma + w2*Mi) + sr1b*(Fa/(Fa + (f8*I10) + s4b2)) +
  A2*T0*(Ma/(Ma+c15)) - k6*I12*T0*(Iy/((Iy*(f1*I4+ f7*I10)) +s1)) -
  k7*T0*(I4/(I4 + f2*Iy + s2)) - MuT0*T0         ;

#Th1 cells (T1)
d/dt(T1) = A3a*(Ma+w2*Mi) + sr3b*(Fa/(Fa+(f8*I10)+s4b1)) +
  k6*I12*T0*(Iy/((Iy*(f1*I4+ f7*I10)) +s1)) - MuTy*(Iy/(Iy+c))*T1*Ma - MuT1*T1 ;

#Th2 cells (T2)
d/dt(T2) = A3a2*(Ma+w2*Mi) + sr3b2*(Fa/(Fa+(f8*I10)+s4b1)) + k7*T0*(I4/(I4+(f2*Iy)+s2)) - MuT2*T2 ;

#Precursor activated CD8+ T cells (T80)
d/dt(T80) = A1a*(Ma+w2*Mi) + sr1b*(Fa/(Fa+(f8*I10)+s4b2)) + A2*T80*(Ma/(Ma+c15)) -
  k6*I12*T80*(Iy/((Iy*(f1*I4+ f7*I10)) +s1)) - MuT80*T80 ;

#Subclass (IFNY producing) of activated CD8+ T cells (T8)
d/dt(T8) = m*A3ac*(Ma+w2*Mi) + m*sr3bc*(Fa/(Fa+(f8*I10)+s4b1)) +
  m*k6*I12*T80*(Iy/((Iy*(f1*I4+ f7*I10)) +s1)) - MuTcy*(Iy/(Iy+cc))*T8*Ma - MuT8*T8 ;

#Subclass (CTL) of activated CD8+ T cells (Tc)
d/dt(Tc) = m*A3ac*(Ma+w2*Mi) + m*sr3bc*(Fa/(Fa+(f8*I10)+s4b1)) +
  m*k6*I12*T80*(Iy/((Iy*(f1*I4+ f7*I10)) +s1)) - MuTcy*(Iy/(Iy+cc))*Tc*Ma - MuTc*Tc ;

#TNF-Alpha
d/dt(Fa) = A30*Mi + A31*Ma*((Iy+(B2*Bt))/(Iy+(B2*Bt)+(f1*I4)+(f7*I10)+s10)) +
  A32*T1 + A33*(Tc+T8) - MuFa*Fa ;

#IFN-Y
#Added impact of AMPK on IFN-y (see S1)
d/dt(Iy) = sg*(Bt/(Bt + c10))*(I12/(I12+s7)) + A5a*T1*(Ma/(Ma+c5b)) +
  A5b*T8*(Ma/(Ma+c5a)) + A7*T0*(I12/(I12+f4*I10+s4)) +
  A7*T80*(I12/(I12 + f4*I10 + s4))  - MuIy*Iy +
  A5c*Mi*(1 - (ImAMPKIy*AMPK_pT172/(I50AMPKIy+AMPK_pT172))) ;
```

```
  #IL-12
  d/dt(I12) = s12*(Bt /(Bt +c230)) + A23*Mr*(Bt /(Bt +c23)) +
    A8*Ma*(s/(s+I10)) - MuI12*I12 ;

  #IL-10
  d/dt(I10) = D7*Ma*(s6/(I10+(f6*Iy)+s6)) + A16*T1 + A17*T2 + A18*(T8+Tc) - MuI10*I10 ;

  #IL-4
  d/dt(I4) = A11*T0 + A12*T2 - MuI4*I4 ;

  #IL1b
  #Added (See S1)
  d/dt(IL1b) = kin1b1*Ma*((Iy+(B2*Bt))/(Iy+(B2*Bt)+f1*I4+(f7*I10)+s10)) - Mu1b*IL1b ;


})
```

2 Parameter Values used in the Simulations

Parameter	Value	Units	Description	Source
A5a	50	pg/Th1 day	IFN–y production by Th1	[Sud2006]
A30	0.003	pg/ml MI day	TNF production by MI	[Sud2006]
A4a	0.005	1/day	TNF-independent recruitment of MR	[Sud2006]
A23	2e-04	pg/ml MR	IL-12 production by MR	[Sud2006]
A5b	50	pg/T8 day	IFN–y production by T8 cells	[Sud2006]
A18	0.02	pg/(CD8 total) day	IL-10 production by TCs and T8s	[Sud2006]
A3a2	0.001	1/day	Th2 recruitment by chemokines	[Sud2006]
A3ac	0.003	1/day	TNF-independent recruitment of TC/T8	[Sud2006]
A31	0.004	pg/ml MA day	TNF production by MA	[Sud2006]
A1a	0.005	1/day	TNF-independent recruitment of Th0	[Sud2006]
A32	0.000816	pg/ml Th1 day	TNF production by Th1	[Sud2006]
A33	6e-05	pg/ml T8 day	TNF production by T8	[Sud2006]
A3a	0.005	1/day	TNF-independent recruitment of Th1	[Sud2006]
sr3b2	1000	1/day	TNF-dependent recruitment of Th2	[Sud2006]
sr4b	20000	MR/day	TNF-dependent recruitment of MR	[Sud2006]
sr1b	2e+05	Th0/day	TNF-dependent recruitment of Th0	[Sud2006]
sr3b	20000	Th1/day	TNF-dependent recruitment of Th1	[Sud2006]
sr3bc	80000	T/day	TNF-dependent recruitment of TC/T8	[Sud2006]
f9	50	Scalar	Ratio adjustment, TNF/IL10	[Sud2006]
f7	1	Scalar	Effect of IL-10 on IFN-induced Th0 to Th1	[Sud2006]
f8	1	Scalar	Ratio adjustment, IL-10/TNF on MR recruitment	[Sud2006]
s4b1	165	pg/ml	recruitment Half-sat, effect of TNF on Th1	[Sud2006]

(continued)

Parameter	Value	Units	Description	Source
s4b2	450	pg/ml	recruitment Half-sat, effect of TNF on Th0 recruitment	[Sud2006]
s4b	200	pg/ml day	Half-sat, TNF on MR recruitment	[Sud2006]
B2	0.001		Scaling factor of BT for TNF production by MA	[Sud2006]
B	100	BT/pg	Scaling factor of TNF for MR to MA	[Sud2006]
c	1100	pg/ml	Half-sat, IFN–y on Th1 death	[Sud2006]
cc	550	pg/ml	Half-sat, IFN–y on TC/T8 death	[Sud2006]
c52	50	TC	Half-sat, TC on MI killing	[Sud2006]
cT1	10	Th1	Half-sat, effect of Th1 on TC cytotoxicity	[Sud2006]
c5a	7e+06	MA	Half-sat, MA on IFN–y by Th1	[Sud2006]
cT	10000	BT	Half-sat, BT on TNF production by Th1/T8	[Sud2006]
c5b	7e+06	MA	Half-sat, MA on IFN–y by T8	[Sud2006]
c230	1e+06	BT	Half-sat, BT on IL-12 by dendritic cells	[Sud2006]
c23	5e+06	BT	Half-sat, BT on IL-12 by MR	[Sud2006]
w3	0.4	unitless	Max percentage contribution by Th1 to Fas-FasL	[Sud2006]
w2	0.15	unitless	Max, percentage contribution of MI-produced chemokines to MR recruitment	[Sud2006]
w1	0.5	unitless	Max percentage contribution of Th1 to cytotoxicity	[Sud2006]
m	0.6	Scalar	Percentage overlap between TC and T8 subsets	[Sud2006]
MuTy	1e-04	1/MA day	IFN- -induced apoptosis rate of Th1	[Sud2006]
MuTcy	1e-04	1/MA day	Th1 IFN- -induced apoptosis rate of TC/T8	[Sud2006]
MuT8	0.33	1/day	T8 death rate	[Sud2006]
MuTc	0.33	1/day	Tc death rate	[Sud2006]
MuT80	0.33	1/day	T80 death rate	[Sud2006]

(continued)

Parameter	Value	Units	Description	Source
MuFa	1.112	1/day	TNF decay rate	[Sud2006]
k14a	0.1	1/day	Fas-FasL-induced apoptosis of MI	[Sud2006]
k14b	0.1	1/day	TNF induced apoptosis of MI	[Sud2006]
k52	0.02	1/day	Cytotoxic killing of MI	[Sud2006] Active disease value
s10	80	pg/ml	Half-sat, IFN–y on TNF production by MA	[Sud2006]
s12	300	pg/ml day	Dendritic cell production of IL-12	[Sud2006]
s	10	pg/ml	Describes IL-10 downregulation of IL-12 by MA	[Sud2006]
D7	0.01	pg/ml MA	IL-10 production by MA	[Sud2006]
Nfraca	0.5	scalar	Average bacteria within a single MI released upon TNF-apoptosis	[Sud2006]
Nfracc	0.1	scalar	Average bacteria within a single MI released upon FAS-apoptosis	[Sud2006]
A201	0.9	1/day	Be growth rate log-phase	optimized
A191	1.9	1/day	BI growth rate log-phsae	optimized
A202	0.05	1/day	Be growth rate slow-phase	[Sud2006] median of range
A192	0.34	1/day	BI growth rate slow-phase	[Sud2006] median of range
A12	0.001	pg/Th2 day	IL-4 production by Th2b	[Sud2006]
A11	5e-04	pg/Th0 day	IL-4 production by Th0b	[Sud2006]
A17	0.06	pg/Th2 day	IL-10 production by Th2b	[Sud2006]
A8	8e-05	pg/MA day	IL-12 production by MAb	[Sud2006]
A7	0.03	pg/ml Th0	IFN–y production by Th0b	[Sud2006]
A16	0.002	pg/Th1 day	IL-10 production by Th1b	[Sud2006]

(continued)

Parameter	Value	Units	Description	Source
A2	0.005	1/day	Max growth rate of Th0b	[Sud2006]
srm	1000	MR/day	MR recruitment rateb	[Sud2006]
f6	0.025	Scalar	Adjustment, IFN–y on IL-10b	[Sud2006]
f4	2	Scalar	Adjustment, IL-10/IL-12 on IFN–yb	[Sud2006]
f2	1	Scalar	Adjustment, IFN–y/IL-4b	[Sud2006]
f1	200	Scalar	Adjustment, IL-4/IFN–yb	[Sud2006]
s2	5	pg/ml	Half-sat, IL-4b	[Sud2006]
s6	60	pg/ml	Half-sat, IL-10 self-inhibition in MAb	[Sud2006]
s4	50	pg/ml	Half-sat, IL-12 on IFNb	[Sud2006]
s7	40	pg/ml	Half-sat, IL-12 on IFN–y by NK cellsb	[Sud2006]
s1	70	pg/ml	Half-sat, IFN–y on MR to MAb	[Sud2006]
s8	1	pg/ml	Half-sat, IL-10 on MA deactivationb	[Sud2006]
c9	2e+06	BE	Half-sat, BE on MR infectionb	[Sud2006]
c8	1e+08	BT	Half-sat, BT on MR activationb	[Sud2006]
c4	40	T/MI	Half-sat, T/MI ratio for MI lysisb	[Sud2006]
c15	2e+05	MA	Half-sat, MA on IFN–y by Th1b	[Sud2006]
c10	1e+06	BT	Half-sat, bacteria on IFN by NK cellsb	[Sud2006]
MuMr	0.011	1/day	Death rate, MR	[Marino2004]
MuMi	0.011	1/day	MI death rate	[Marino2004]
MuMa	0.011	1/day	MA death rate	[Marino2004]
MuIy	3	1/day	IFN–y decay rate	[Marino2004]
MuI4	2.77	1/day	IL-4 decay rateb	[Sud2006]
MuI10	5	1/day	IL-10 decay rateb	[Sud2006]
Mui	0.004	1/day	BI to BE due to MI death	[Sud2006]
MuI12	1.188	1/day	IL-12 decay rateb	[Sud2006]
MuT2	0.33	1/day	Th2 death rateb	[Sud2006]
MuT1	0.33	1/day	Th1 death rateb	[Sud2006]
MuT0	0.33	1/day	Th0 death rateb	[Sud2006]
k2	0.4	1/day	MR infection rateb	[Sud2006]
k3	0.1	1/day	MR activation rateb	[Sud2006]
k17	0.1	1/day	Max. MI death due to BIb	[Marino2010]

(continued)

Parameter	Value	Units	Description	Source
k4	0.08	1/day	MA deactivation by IL-10b	[Sud2006]
k6	0.005	ml/pg day	Max Th0 to Th1 rateb	[Sud2006]
k7	0.02	ml/pg day	Max Th0 to Th2 rateb	[Sud2006]
k18	5e-09	ml/MR day	BE killing by MRb	[Sud2006]
k15	1.25e-07	ml/MA day	BE killing by MAb	[Sud2006]
A5c	0.03	1/day	Mi production of IFN-y	[Sud2006]
sg	100	pg/ml day	IFN-y production by NK cells	[Sud2006]
N	20	BI/MI	Carrying capacity of infected macrophages (Marino 2004)	[Sud2006]
Mu1b	2.112	1/day	Decay rate of IL-1b	Dai 2020
k14x	0.12	1/day	IL1b driven macrophage apoptosis rate	optimized
s4x	2700	pg/mL	Il1b EC50 macrophage apoptosis	optimized
kin1b1	0.3	1/day	calculated based on SS IL1b value in TB patients	calculated
P1	178.9531	1/day	IR beta phosphorylation by Insulin	[Sonntag2012]
P2	570.5784	1/day	IR beta pY1146 dephosphorylation	[Sonntag2012]
P3	76.71888	1/day	IR beta ready	[Sonntag2012]
P4	7.079026	1/day	IRS1 phosphorylation by IR beta pY1146	[Sonntag2012]
P5	2423160	1/day	IRS1 p phosphorylation by p70S6K pT389	[Sonntag2012]
P6	18.792	1/day	IRS1 pS636 dephosphorylation	[Sonntag2012]
P7	14108.63	1/day	AMPK T172 phosphorylation	[Sonntag2012]
P8	15.43896	1/day	AMPK pT172 dephosphorylation	[Sonntag2012]
P9	4.831848	1/day	Akt pT308 dephosphorylation	[Sonntag2012]
P10	9.21911	1/day	Akt pS473 dephosphorylation	[Sonntag2012]
P11	18927.65	1/day	Akt S473 phosphorylation by mTORC2 pS2481 n IRS1 p	[Sonntag2012]

(continued)

Parameter	Value	Units	Description	Source
P12	9962.078	1/day	Akt T308 phosphorylation by IRS1 p = 6.91811	[Sonntag2012]
P13	15.35789	1/day	mTORC1 pS2448 dephosphorylation by TSC1 TSC2 pS1387	[Sonntag2012]
P14	6.32039	1/day	mTORC1 S2448 activation by Amino Acids	[Sonntag2012]
P15	26.45784	1/day	mTORC2 pS2481 dephosphorylation	[Sonntag2012]
P16	540.5083	1/day	mTORC2 S2481 phosphorylation by PI3K variant p	[Sonntag2012]
P17	16.34573	1/day	p70S6K pT389 dephosphorylation	[Sonntag2012]
P18	2.650219	1/day	p70S6K T389 phosphorylation by mTORC1 pS2448	[Sonntag2012]
P19	3355.402	1/day	PRAS40 pS183 dephosphorylation	[Sonntag2012]
P20	1440	1/day	PRAS40 pT246 dephosphorylation	[Sonntag2012]
P21	270.1742	1/day	PRAS40 S183 phosphorylation by mTORC1 pS2448	[Sonntag2012]
P22	198.3298	1/day	PRAS40 T246 phosphorylation by Akt pT308	[Sonntag2012]
P23	52.64482	1/day	TSC1 TSC2 S1387 phosphorylation by AMPK pT172	[Sonntag2012]
P24	25.56893	1/day	TSC1 TSC2 T1462 phosphorylation by Akt pT308	[Sonntag2012]
P25	14400	1/day	PI3K variant p dephosphorylation	[Sonntag2012]
P26	14.4	1/day	PI3K variant phosphorylation by IR beta pY1146	[Sonntag2012]
S50torauto	7	arbitrary unit	SC50 of autophagy inhibition due to mTORC1 phosphorylation	Arbitrary median from simulated range from [Sonntag2012] model

(continued)

Parameter	Value	Units	Description	Source
Smtorauto	100	% change	Smax of autophagy inhibition due to mTORC1 phosphorylation	optimized
kautop	0.004	1/day	Autophagy-mediated Bi elimination rate	optimized
ImAMPKIy	0.6	fold change	Imax of Mi-mediated IFN-y production due to AMPK phosphorylation	Meares 2013 approximate
I50AMPKIy	0.06	arbitrary unit	IC50 of Mi-mediated IFN-y production due to AMPK phosphorylation	Arbitrary median from simulated range from [Sontag2012] model
SLPk2autop	1	unitless	slope of stimulation of Be engulfment into Bi due to autophagy	Arbitrary
VpMET	3	L	Plasma blood volume	[Peters2012]
Vl	1	L	Lung volume	[Peters2012]
Voth	66	L	70 - Vp - Vl other tissue's volume	calculated
Qco	282	L/hr	Cardiac output	[Peters2012]
Kplung	3	unitless	Partition coeff lung to blood plasma for metformin	Zake 2021
CL	52.6	L/hr	Clearance for metformin	Chae 2021
ka	0.4	1/hr	Absorption rate for metformin	[Chae2012]
FRC	1	unitless	fraction going to rest of body optimized using metformin PK data	optimized
Kpoth	1.64	unitless	Partition coeff blood plasma to rest of the body optimized using metformin PK data	optimized
E50MET	50	uM	EC50 of Metformin inhibition of mTORC1	[Hawley2002]
EMMET	0.5	fold-change	EMAX of Metformin inhibition of mTORC1	[Hawley2002]
kmaxiI1	0.05	1/hr	Isoniazid PD max kill rate intracellular day 1	[Fors2020]
kmaxiI2	0.02	1/hr	Isoniazid PD max kill rate intracellular day 2-15	[Fors2020]

(continued)

Parameter	Value	Units	Description	Source
kmaxiI15	0.01	1/hr	Isoniazid PD max kill rate intracellular day >15	[Fors2020]
kmaxeI1	0.4	1/hr	Isoniazid PD max kill rate extracellular day 1	[Fors2020]
kmaxeI2	0.2	1/hr	Isoniazid PD max kill rate extracellular day 2-15	[Fors2020]
kmaxeI15	0.1	1/hr	Isoniazid PD max kill rate extracellular day >15	[Fors2020]
GI	1.05	unitless	Isoniazid PD gamma bactericidal	[Fors2020]
GI1	1.05	unitless	Isoniazid PD gamma bacteriostatic	[Fors2020]
kmaxiR1	0.5	1/hr	Rifampin PD max kill rate intracellular day 1	[Fors2020]
kmaxiR2	0.5	1/hr	Rifampin PD max kill rate intracellular day 2-15	[Fors2020]
kmaxiR15	0.4	1/hr	Rifampin PD max kill rate intracellular day >15	[Fors2020]
kmaxeR1	0.5	1/hr	Rifampin PD max kill rate extracellular day 1	[Fors2020]
kmaxeR2	0.5	1/hr	Rifampin PD max kill rate extracellular day 2-15	[Fors2020]
kmaxeR15	0.4	1/hr	Rifampin PD max kill rate extracellular day >15	[Fors2020]
GR	0.79	unitless	Rifampin PD gamma bactericidal	[Fors2020]
GR1	0.36	unitless	Rifampin PD gamma bacteriostatic	[Fors2020]
kmaxiP1	0	1/hr	Pyrazinamide PD max kill rate intracellular day 1	[Fors2020]
kmaxiP2	0.04	1/hr	Pyrazinamide PD max kill rate intracellular day 2-15	[Fors2020]
kmaxiP15	0.04	1/hr	Pyrazinamide PD max kill rate intracellular day >15	[Fors2020]
kmaxeP1	0	1/hr	Pyrazinamide PD max kill rate extracellular day 1	[Fors2020]

(continued)

Parameter	Value	Units	Description	Source
kmaxeP2	0.02	1/hr	Pyrazinamide PD max kill rate extracellular day 2-15	[Fors2020]
kmaxeP15	0.02	1/hr	Pyrazinamide PD max kill rate extracellular day >15	[Fors2020]
GP	1.21	unitless	Pyrazinamide PD gamma bactericidal	[Fors2020]
GP1	1.21	unitless	Pyrazinamide PD gamma bacteriostatic	[Fors2020]
kmaxiE1	0.05	1/hr	Ethambutol PD max kill rate intracellular day 1	[Fors2020]
kmaxiE2	0.04	1/hr	Ethambutol PD max kill rate intracellular day 2-15	[Fors2020]
kmaxiE15	0.03	1/hr	Ethambutol PD max kill rate intracellular day >15	[Fors2020]
kmaxeE1	0.05	1/hr	Ethambutol PD max kill rate extracellular day 1	[Fors2020]
kmaxeE2	0.04	1/hr	Ethambutol PD max kill rate extracellular day 2-15	[Fors2020]
kmaxeE15	0.03	1/hr	Ethambutol PD max kill rate extracellular day >15	[Fors2020]
GE	1	unitless	Ethambutol PD gamma bactericidal	[Fors2020]
GE1	1	unitless	Ethambutol PD gamma bacteriostatic	[Fors2020]
EC50P	100	mg/L	Pyrazinamide PD	[Fors2020]
EC50P1	50	mg/L	Pyrazinamide PD	[Fors2020]
EC50E	4	mg/L	Ethambutol PD	[Fors2020]
EC50E1	1	mg/L	Ethambutol PD	[Fors2020]
EC50R	5	mg/L	Rifampin PD	[Fors2020]
EC50R1	1.5	mg/L	Rifampin PD	[Fors2020]
EC50I	0.4	mg/L	Isoniazid PD	[Fors2020]
EC50I1	0.1	mg/L	Isoniazid PD	[Fors2020]
VmaxRIF	525	mg/h/70kg	Rifampin max elimination rate	[Svensson2018]
KmRIF	35.3	mg/L	Rifampin Km Elimination	[Svensson2018]
VRIF	87.2	L/70kg	Rifampin Vol distr	[Svensson2018]
kaRIF	1.77	1/hr	Rifampin absorption rate constant	[Svensson2018]
MTTRIF	0.513	hr	Rifampin mean transit time	[Svensson2018]

(continued)

Parameter	Value	Units	Description	Source
NNRIF	23.8	unitless	Rifampin number of transit compartments	[Svensson2018]
EmIRIF	1.16	unitless	Rifampin max increase in enzy production	[Svensson2018]
EC50IRIF	0.0699	mg/L	Rifampin EC50 for enzyme induction	[Svensson2018]
KENZRIF	0.00603	1/hr	Rifampin FO enzyme turnover	[Svensson2018]
FMAXRIF	0.504	unitless	Rifampin Max increase in bioavail above 450 mg	[Svensson2018]
ED50RIF	67	mg	Rifampin Diff in dose from 450 mg at which half Fmax occurs	[Svensson2018]
IIV_VmaxRIF	30	%	IIV Vmax RIF	[Svensson2018]
IIV_KmRIF	35.8	%	IIV Km RIF	[Svensson2018]
IIV_VRIF	7.86	%	IIV V RIF	[Svensson2018]
IIV_kaRIF	33.8	%	IIV ka RIF	[Svensson2018]
IIV_MTTRIF	38.2	%	IIV mtt RIF	[Svensson2018]
IIV_NNRIF	77.9	%	IIV NN RIF	[Svensson2018]
ELFRIF	1.97	unitless	Rifampin ELF to plasma ratio	McCallum 2020
ACRIF	1.35	unitless	Rifampin alveolar cells to plasma ratio	McCallum 2020
CLRINH	26.1	L/hr/52kg	Isoniazid clearance rapid/inter acetylators	[Denti2015]
CLSINH	15.5	L/hr/51.9kg52kg	Isoniazid clearance slow acetylators	[Denti2015]
VINH	48.2	L/52kg	Isoniazid vol distr central	[Denti2015]
QINH	16.1	L/hr/52kg	Isoniazid intercompartmental clearance	[Denti2015]
V2INH	16.5	L	Isoniazid vol distr peripheral	[Denti2015]
MTTINH	0.924	hr	Isoniazid mean transit time	[Denti2015]
NNINH	2.73	unitless	Isoniazid number of transit cmt	[Denti2015]
IIV_CLINH	30.7	%	IIV CL INH	[Denti2015]
IIV_MTTINH	37.4	%	IIV MTT INH	[Denti2015]
ELFINH	14.6	unitless	Isoniazid ELF to plasma ratio	McCallum 2020
ACINH	1.31	unitless	Isoniazid alveolar cells to plasma ratio	McCallum 2020
CLPYZ	3.32	L/hr/51.9kg52kg	Pyrazinamide clearance	[Denti2015]
VPYZ	40.1	L/52kg	Pyrazinamide vol dist	[Denti2015]

(continued)

Parameter	Value	Units	Description	Source
MTTPYZ	0.84	hr	Pyrazinamide mean transit time	[Denti2015]
NNPYZ	2.6	unitless	Pyrazinamide number of transit cmt	[Denti2015]
CLI2M	16.3	%	Increase in CL after 2 month treatment	[Denti2015]
IIV_CLPYZ	22.6	%	IIV CL PYZ	[Denti2015]
ELFPYZ	49.8	unitless	Pyrazinamide ELF to plasma ratio	McCallum 2020
ACPYZ	3.18	unitless	Pyrazinamide alveolar cells to plasma ratio	McCallum 2020
CLETH	40.7	L/hr/51.9kg52kg	Ethambutol clearance	[Denti2015]
VETH	266	L/52kg	Ethambutol vol dist	[Denti2015]
QETH	109	L/hr/51.9kg52kg	Ethambutol intercompartmental clearance	[Denti2015]
V2ETH	687	L/52kg	Ethambutol vol dist peri	[Denti2015]
MTTETH	2.54	hr	Ethambutol mean transit time	[Denti2015]
NNETH	11.1	unitless	Ethambutol number of transit cmt	[Denti2015]
AGECLETH	-1.41	% per yr	Effect on age on ethambutol CL	[Denti2015]
ELFETH	4	unitless	Ethambutol ELF to plasma ratio	McCallum 2020
ACETH	15	unitless	Ethambutol alveolar cells to plasma ratio	McCallum 2020

Note:
[Sud2006]=[6]
[Marino2004]=[18]
[Marino2010]=[19]
[Dai2021]=[7]
[Sonntag2012]=[13]
[Lachmandas2019]=[17]
[Sonntag2012]=[13]
[Peters2012]=[20]
[Zake2021]=[**?**]
[Chae2012]=[21]
[Fors2020]=[12]
[Svensson2018]=[1]
[McCallum2021]=[3]
[Denti2015]=[2]

3 Uncertainty and Sensitivity Analysis: Parameters Affecting Total Bacterial Load

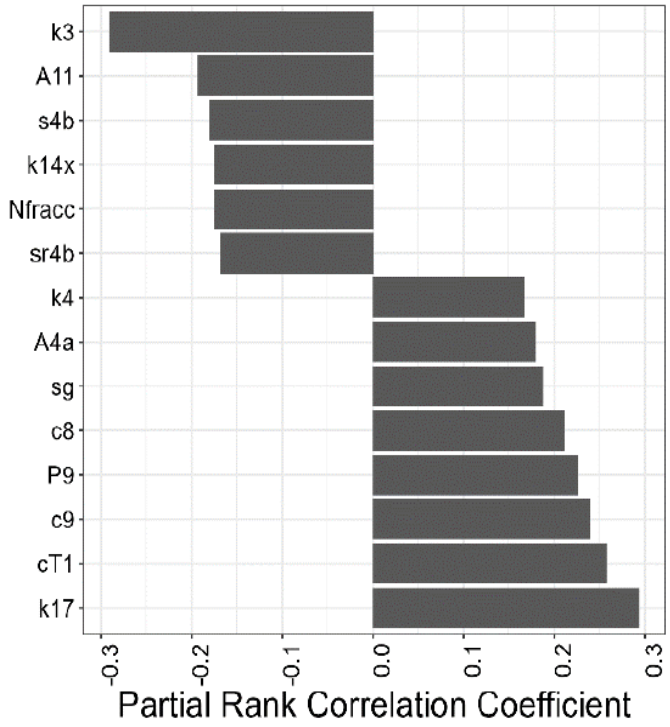

A11=IL-4 production by T-helper cells, A4a=TNF-independent recruitment of resident macrophage, c8= half-saturation levels of effects of total bacterial on resident macrophage activation, c9=half-sat levels of extracellular bacteria on extracellular to intracellular bacterial uptake, cT1=half-sat levels for effect of T-helper cells on cytotoxic lymphocytes activity, k14x=IL-1b driven macrophage apoptosis rate, k17=max macrophage death due to intracellular bacteria, k3=macrophage activation rate, k4=activated macrophage deactivation by IL-10, Nfracc=average bacteria released upon FAS-FAS-apoptosis, P9=Akt dephosphorylation rate, sg=IFN-γ production by NK cells, sr4b=TNF-dependent recruitment of resident macrophage, s4b=half-sat levels for TNF on resident macrophage recruitment

References

[1] Svensson EM, Svensson RJ, te Brake LHM, Boeree MJ, Heinrich N, Konsten S, et al. The Potential for Treatment Shortening With Higher Rifampicin Doses: Relating Drug Exposure to Treatment Response in Patients With Pulmonary Tuberculosis. Clinical Infectious Diseases. 2018 03;67(1):34-41.

[2] Denti P, Jeremiah K, Chigutsa E, Faurholt-Jepsen D, PrayGod G, Range N, et al. Pharmacokinetics of Isoniazid, Pyrazinamide, and Ethambutol in Newly Diagnosed Pulmonary TB Patients in Tanzania. PLOS ONE. 2015 10;10(10):1-19. Available from: https://doi.org/10.1371/journal.pone.0141002.

[3] McCallum AD, Pertinez HE, Else LJ, Dilly-Penchala S, Chirambo AP, Sheha I, et al. Intrapulmonary Pharmacokinetics of First-line Anti-tuberculosis Drugs in Malawian Patients With Tuberculosis. Clinical Infectious Diseases. 2020 08;73(9):e3365-73. Available from: https://doi.org/10.1093/cid/ciaa1265.

[4] Jermain B, Hanafin P, Cao Y, Lifschitz A, Lanusse C, GG R. Development of a Minimal Physiologically-Based Pharmacokinetic Model to Simulate Lung Exposure in Humans ollowing Oral Administration of Ivermectin for COVID-19 Drug Repurposing. J Pharm Sci. 2020;109(12):3574-8.

[5] Zake DM, Kurlovics J, Zaharenko L, Komasilovs V, Klovins J, Stalidzans E. Physiologically based metformin pharmacokinetics model of mice and scale-up to humans for the estimation of concentrations in various tissues. PLOS ONE. 2021 04;16(4):1-27. Available from: https://doi.org/10.1371/journal.pone.0249594.

[6] Sud D, Bigbee C, Flynn JL, Kirschner DE. Contribution of CD8+ T Cells to Control of Mycobacterium tuberculosis Infection. The Journal of Immunology. 2006;176(7):4296-314.

[7] Dai W, Rao R, Sher A, Tania N, Musante CJ, Allen R. A Prototype QSP Model of the Immune Response to SARS-CoV-2 for Community Development. CPT: Pharmacometrics & Systems Pharmacology. 2021;10(1):18-29.

[8] Casarini M, Amegli F, Alemanno L, Zangrilli P, Mattia P, Paone G, et al. Cytokine Levels Correlate with a Radiologic Score in Active Pulmonary Tuberculosis. American Journal of Respiratory and Critical Care Medicine. 1999;159(1):143-8. PMID: 9872832.

[9] Jayaraman P, Sada-Ovalle I, Nishimura T, Anderson AC, Kuchroo VK, Remold HG, et al. IL-1?? Promotes Antimicrobial Immunity in Macrophages by Regulating TNFR Signaling and Caspase-3 Activation. The Journal of Immunology. 2013;190(8):4196-204.

[10] Reiling N, Hölscher C, Fehrenbach A, Kröger S, Kirschning CJ, Goyert S, et al. Cutting Edge: Toll-Like Receptor (TLR)2- and TLR4-Mediated Pathogen Recognition in Resistance to Airborne Infection with Mycobacterium tuberculosis. The Journal of Immunology. 2002;169(7):3480-4.

[11] Musuka S, Srivastava S, Dona CWS, Meek C, Leff R, Pasipanodya J, et al. Thioridazine Pharmacokinetic-Pharmacodynamic Parameters “Wobble” during Treatment of Tuberculosis: a Theoretical Basis for Shorter-Duration Curative Monotherapy with Congeners. Antimicrobial Agents and Chemotherapy. 2013;57(12):5870-7.

[12] Fors J, Strydom N, Fox WS, Keizer RJ, Savic RM. Mathematical model and tool to explore shorter multi-drug therapy options for active pulmonary tuberculosis. PLOS Computational Biology. 2020 08;16(8):1-36. Available from: https://doi.org/10.1371/journal.pcbi.1008107.

[13] Sonntag AG, Dalle Pezze P, Shanley DP, Thedieck K. A modelling-experimental approach reveals insulin receptor substrate (IRS)-dependent regulation of adenosine monosphosphate-dependent kinase (AMPK) by insulin. The FEBS Journal. 2012;279(18):3314-28.

[14] Singhal A, Jie L, Kumar P, Hong GS, Leow MKS, Paleja B, et al. Metformin as adjunct antituberculosis therapy. Science Translational Medicine. 2014;6(263):263ra159-9.

[15] Hawley SA, Gadalla AE, Olsen GS, Hardie DG. The Antidiabetic Drug Metformin Activates the AMP-Activated Protein Kinase Cascade via an Adenine Nucleotide-Independent Mechanism . Diabetes. 2002 08;51(8):2420-5. Available from: https://doi.org/10.2337/diabetes.51.8.2420.

[16] Howell JJ, Hellberg K, Turner M, Talbott G, Kolar MJ, Ross DS, et al. Metformin Inhibits Hepatic mTORC1 Signaling via Dose-Dependent Mechanisms Involving AMPK and the TSC Complex. Cell Metabolism. 2017;25(2):463-71.

[17] Lachmandas E, Eckold C, Böhme J, Koeken VACM, Marzuki MB, Blok B, et al. Metformin Alters Human Host Responses to Mycobacterium tuberculosis in Healthy Subjects. The Journal of Infectious Diseases. 2019 02;220(1):139-50. Available from: https://doi.org/10.1093/infdis/jiz064.

[18] Marino S, Kirschner DE. The human immune response to Mycobacterium tuberculosis in lung and lymph node. Journal of Theoretical Biology. 2004;227(4):463-86.

[19] Marino S, Myers A, Flynn JL, Kirschner DE. TNF and IL-10 are major factors in modulation of the phagocytic cell environment in lung and lymph node in tuberculosis: A next-generation two-compartmental model. Journal of Theoretical Biology. 2010;265(4):586-98.

[20] Appendices. In: Physiologically-Based Pharmacokinetic (PBPK) Modeling and Simulations. John Wiley; 2012. p. 407-21.

[21] Chae Jw, Baek Ih, Lee By, Cho Sk, Kwon Ki. Population PK/PD analysis of metformin using the signal transduction model. British Journal of Clinical Pharmacology;74(5):815-23.